Synthetic and Systems Biotechnology 7 (2022) 756–764

Contents lists available at ScienceDirect

Synthetic and Systems Biotechnology

journal homepage: www.keaipublishing.com/en/journals/synthetic-and-systems-biotechnology

Original Research Article

Multi-strategy engineering unusual sugar TDP-L-mycarose biosynthesis to improve the production of 3-*O*-*α*-mycarosylerythronolide B in *Escherichia coli*

Zhifeng Liu [a,b,1], Jianlin Xu [a,b,c,1], Zhanguang Feng [a,b], Yong Wang [a,*]

[a] CAS-Key Laboratory of Synthetic Biology, CAS Centre for Excellence in Molecular Plant Sciences, Institute of Plant Physiology and Ecology, Chinese Academy of Sciences, Shanghai, 200032, China
[b] University of Chinese Academy of Sciences, Beijing, 100039, China
[c] State Key Laboratory of Bioreactor Engineering, East China University of Science and Technology, Shanghai, 200237, China

ARTICLE INFO

Keywords:
TDP-L-mycarose
Glycosylated products
3-*O*-*α*-mycarosylerythronolide B
Metabolic engineering
CRISPRi

ABSTRACT

The insufficient supply of sugar units is the key limitation for the biosynthesis of glycosylated products. The unusual sugar TDP-L-mycarose is initially attached to the C3 of the polyketide erythronolide B, resulting in 3-*O*-*α*-mycarosylerythronolide B (MEB). Here, we present the de novo biosynthesis of MEB in *Escherichia coli* and improve its production using multi-strategy metabolic engineering. Firstly, by blocking precursor glucose-1-phosphate competing pathways, the MEB titer of triple knockout strain QC13 was significantly enhanced to 41.2 mg/L, 9.8-fold to that produced by parental strain BAP230. Subsequently, the MEB production was further increased to 48.3 mg/L through overexpression of *rfbA* and *rfbB*. Moreover, the CRISPRi was implemented to promote the TDP-L-mycarose biosynthesis via repressing the glycolysis and TDP-L-rhamnose pathway. Our study paves the way for efficient production of erythromycins in *E. coli* and provides a promising platform that can be applied for biosynthesis of other glycosylated products with unusual sugars.

1. Introduction

Glycosylated natural products have diverse bioactivity and improved properties, which are closely associated with the structure and attachment pattern of the sugar units [1,2]. It has been well explored that the sugar moiety of many therapeutic agents participates in the interaction between the drug and cellular target which enables effective drug targeting and improved pharmacological properties [3–7].

Typically, the sugar units were originated from nucleoside diphosphate (NDP)-sugars, which can be categorized into distinct groups according to the complexity of biosynthetic pathway, namely common sugars and unusual sugars. Common sugars such as UDP-glucose and TDP-glucose are directly synthesized from sugar-1-phosphate (mainly glucose-1-phosphate, G1P) under the catalysis of nucleotidylyltransferase. Highly modified unusual sugars are generated through multi-step decorations including the epimerization, deoxygenation, ketoreduction and *C*-, *N*-, or *O*-methylations of common precursor TDP-4-keto-6-deoxy-D-glucose (TKDG), the immediate product of TDP-glucose catalyzed by TDP-4,6-dehydratase, which contribute to the formation of structurally diverse natural glycosylated compounds. In recent years, pathway modification and/or combinatorial biosynthesis has emerged as a promising strategy to generate various unusual sugars and novel glycosylated compounds with enhanced activities [8–10]. For example, by the inactivation of native gene *dnrV* and the expression of heterologous gene *avrB* or *eryBIV*, the TDP-L-daunosamine biosynthetic pathway of *Streptomyces peucetius* was modified to produce TDP-4′-*epi*-L-daunosamine that was the epimer at C4′ hydroxyl group of TDP-L-daunosamine, and the resulting glycosylated product epirubicin (4′-epidoxorubicin) possessed more effective antitumor property [11]. Besides, a series of undescribed deoxysugars were synthesized and attached to the anthracycline aglycones, resulting in the generation of unusual anthracycline analogues [12].

Nevertheless, the biosynthesis of complex glycosylated products is usually hampered attributable to the insufficient availability of sugar

Peer review under responsibility of KeAi Communications Co., Ltd.
* Corresponding author. .
E-mail address: yongwang@cemps.ac.cn (Y. Wang).
[1] These authors contribute equally to this work.

https://doi.org/10.1016/j.synbio.2022.03.002
Received 30 January 2022; Received in revised form 9 March 2022; Accepted 13 March 2022

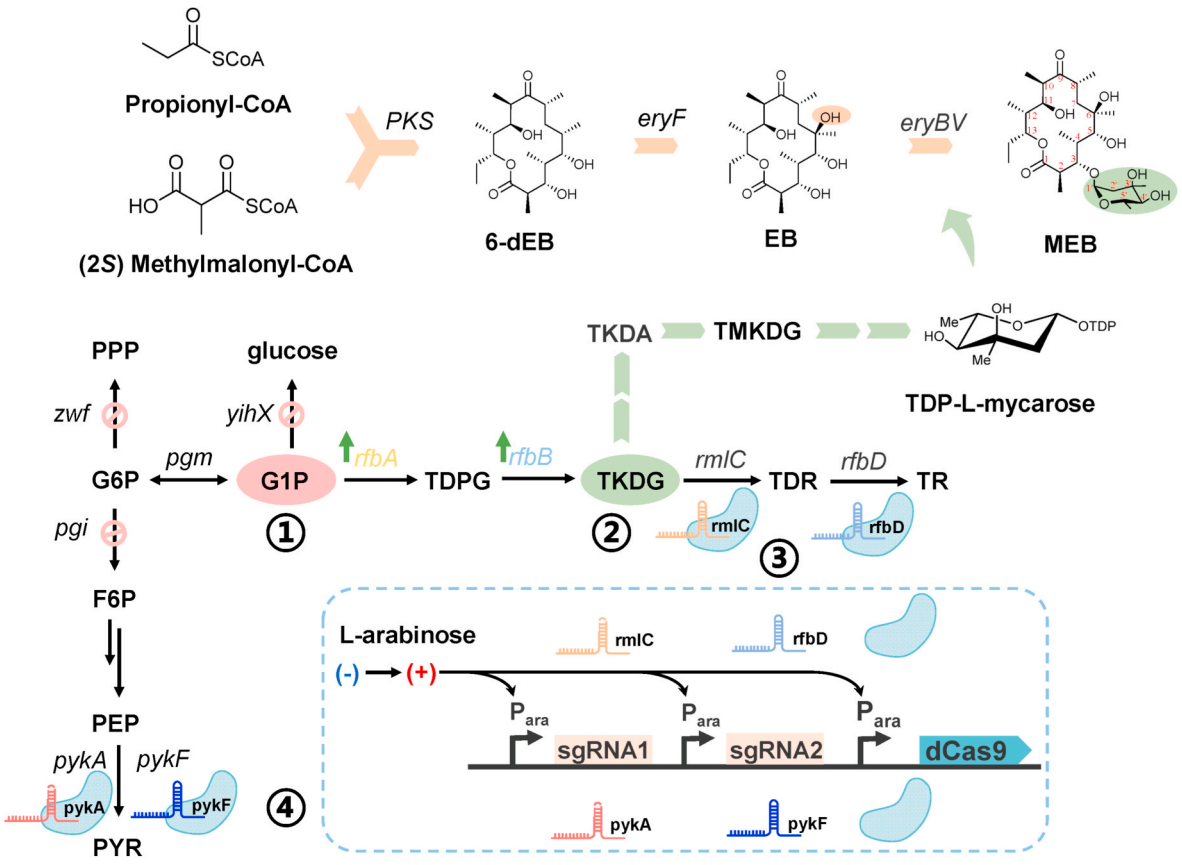

Fig. 1. Metabolic strategies for improving the 3-*O*-*α*-mycarosylerythronolide B (MEB) production in *E. coli*. The scheme represents key metabolic pathways, metabolites and genes involved in the biosynthesis of MEB. Orange-coloured arrows indicate the main metabolic pathways of MEB; black-coloured arrows indicate the native metabolic pathways in *E. coli*; green-coloured arrows indicate the overexpression of the heterologous TDP-L-mycarose from *Saccharopolyspora erythraea;* the blue rectangle with dash line indicate the CRISPRi system based on L-arabinose. the pink circles indicate deletion of the genes; the green up arrows indicate the overexpression of genes; 6-dEB, 6-deoxyerythronolide B; EB, erythronolide B; MEB, 3-*O*-*α*-mycarosylerythronolide B; PPP, pentose phosphate pathway; G6P, glucose-6-phosphate; F6P, fructose-6-phosphate; PEP, phosphoenolpyruvate; PYR, pyruvate; G1P, glucose-1-phosphate; TDPG, TDP-glucose; TKDG, TDP-4-keto-6-deoxy-D-glucose; TDR, TDP-4-dehydro-L-rhamnose; TR, TDP-L-rhamnose; TKDA, TDP-4-oxo-2,6-dideoxy-D-allose; TMKDG, TDP-3-methyl-4-oxo-2,6-dideoxy-D-glucose; *PKS*, polyketide synthetase; *eryF*, C6-hydroxylase; *eryBV*, L-mycarosyltransferase; *zwf*, glucose-6-phosphate dehydrogenase; *pgi*, phosphoglucose isomerase; *pykA*, pyruvate kinase II; *pykF*, pyruvate kinase I; *pgm*, phosphoglucomutase; *yihX*, *α*-D-glucose-1-phosphate phosphatase; *rfbA*, glucose-1-phosphate thymidylyltransferase; *rfbB*, dTDP-glucose-4,6-dehydratase; *rmlC*, TDP-4-dehydrorhamnose-3,5-epimerase; *rfbD*, TDP-L-rhamnose synthase.

units in the heterologous host [13–15]. Several metabolic engineering approaches including overexpression of endogenous genes [16], deletion of competitive pathways [17], the introduction of heterologous pathway genes [18], and reconstruction of independent pathways from other carbon resources [19,20] have been widely employed to enhance the production of glycosides conjugated with UDP-glucose. Though attempts have been made to increase the supply of precursor G1P via engineering the metabolic pathway of *streptomyces* [21–23], metabolic engineering *Escherichia coli* to enhance the unusual sugar pool has been scarcely reported.

Erythromycin A, the 14-membered macrocyclic lactone attached with two unusual sugar units TDP-L-mycarose and TDP-D-desosamine that are the fundamental determinants for its antibacterial activity, is the representative member of polyketides used as an antibacterial drug in clinical treatment. Despite the fact that the production of polyketide skeleton erythronolide B (EB) reached 180 mg/L in *E. coli* [24], the yield of downstream erythromycins was extremely low. For example, the heterologous expression of 17 genes encoding two unusual monosaccharide biosynthetic enzymes enabled the 6-dEB-producing *E. coli* to generate erythromycins C and D with titers of 0.4 and 0.5 mg/L, respectively [25]. When introducing the whole erythromycin biosynthesis genes into *E. coli* and performing the two-step fermentation, the yield of the final product erythromycin A just reached 0.6 mg/L [26]. Additionally, Jiang et al. reconstructed the plasmids that contained the entire erythromycin biosynthetic gene cluster, resulting in the production of 1.2 mg/L erythromycin A [27]. The possible reason that the titer of erythromycins in *E. coli* is low might be attributed to the insufficient supply of two unusual sugars. It has been demonstrated that deletion of three genes (*WecE*, *VioA*, and *RmlC*) in the TKDG consumed pathway, the genetically modified strains strengthened the biosynthesis of TDP-L-mycarose and TDP-D-desosamine and was able to transform 6-dEB into erythromycin D, 60-fold to that of the original strain [28]. While the reported biocatalysts of 6-dEB necessitate further improvement to support the high production of erythromycin, there have been rare efforts to investigate and optimize the de novo microbial biosynthesis of 3-*O*-*α*-mycarosylerythronolide B (MEB), the first glycosylated intermediator of erythromycin.

In this study, we establish the de novo MEB biosynthesis in *E. coli* and present a more comprehensive approach to promote the yield of MEB (Fig. 1). To achieve this, the bypass pathway of G1P was initially blocked (strategy 1). Then, key enzymes of the metabolic pathway were overexpressed to facilitate the biosynthesis of TKDG (strategy 2). Next, genes *rmlC* and *rfbD* were repressed to redirect the metabolic flux toward the TDP-L-mycarose via CRISPRi (strategy 3). Furthermore, repression of the glycolysis pathway was applied to enhance the endogenous TDP-L-mycarose pool and facilitate MEB concentration (strategy 4).

Table 1
Plasmids and strains used in this research.

Plasmids/ Strains	Description	Source
Plasmids		
pBP130	pET21c-PT7-*DEBS2-DEBS3*-T7ter	29
pBP144	pET28a-PT7-*pccB*-rbs-*pccA*-PT7-*DEBS1*-T7ter	29
pJF26	pET21c-PT7-*eryBVI*-T7ter	Lab stock
pJF27	pET21c-PT7-*eryBII*-T7ter	Lab stock
pJF28	pET21c-PT7-*eryBVII*-T7ter	Lab stock
pJF29	pET21c-PT7-*eryBIII*-T7ter	Lab stock
pJF30	pET21c-PT7-*eryBIV*-T7ter	Lab stock
pJF31	pET21c-PT7-*eryBV*-T7ter	Lab stock
pJF33	pET21c-PT7-*eryBVII-eryBIII*-T7ter	Lab stock
pJF35	pET21c-PT7-*ermE*-T7ter	Lab stock
pJF37	pET21c-PT7-*eryBIV-eryBV-ermE*-T7ter	Lab stock
pZF90	pET21c-PT7-*AeeryBIII*-T7ter	This study
pZF91	pET21c-PT7-*AeeryBVII*-T7ter	This study
pZF92	pET21c-PT7-*AeeryBVII-AeeryBIII*-T7ter	This study
pZF93	pCDFDuet-PT7-*SaeryF-GroESL*-T7ter	This study
pZF94	pET21c-PT7-*eryBVI-eryBII*-T7ter	This study
pZF95	pCDFDuet-PT7-*SaeryF-GroESL-eryBVI-eryBII*-T7ter	This study
pZF223	pET21c-PT7-*GroESL*-T7ter	This study
pZF225	pET21c-PT7-*EcrfbB-EcrfbA*-T7ter	This study
pZF227	pCDFDuet-PT7-*SaeryF-GroESL-eryBVI-eryBII-eryBVII-eryBIII*-T7ter	This study
pZF228	pCDFDuet-PT7-*SaeryF-GroESL-eryBVI-eryBII-AeeryBVII-AeeryBIII*-T7ter	This study
pZF229	pCDFDuet-PT7-*SaeryF-GroESL-eryBVI-eryBII-eryBVII-eryBIII-eryBIV-eryBV-ermE*-T7ter	This study
pZF230	pCDFDuet-PT7-*SaeryF-GroESL-eryBVI-eryBII-AeeryBVII-AeeryBIII-eryBIV-eryBV-ermE*-T7ter	This study
pZF234	pZF230-*rfbB-rfbA*	This study
pZF208	pACYC-sgRNA_Plux	Lab stock
pACYC-dCas9-Ter	dcas9 expression plasmid	Lab stock
pZF236	pACYC-sgRNA_Para	This study
pZF237	pZF236_pykA_N20	This study
pZF238	pZF236_pykF_N20	This study
pZF239	pACYC-*dcas9*-ter_sgRNA_pykA_sgRNA_pykF	This study
pZF243	pZF236_rmlC_N20	This study
pZF244	pZF236_rfbD_N20	This study
pZF246	pACYC-*dcas9*-ter_sgRNA_rmlC_sgRNA_rfbD	This study
Strains		
BAP1	F-ompT hsdSB (rB-mB-) gal dcm (DE3) prpRBCD::PT7-sfp, PT7-prpE	29
WT	BAP1 carrying pBP130, pBP144	This study
BAP93	BAP1 carrying pBP130, pBP144, pZF93	This study
BAP229	BAP1 carrying pBP130, pBP144, pZF229	This study
BAP230	BAP1 carrying pBP130, pBP144, pZF230	This study
ZF1	BAP1Δ*pgi*	This study
ZF2	BAP1Δ*zwf*	This study
ZF3	BAP1Δ*yihX*	This study
ZF7	BAP1Δ*pgi*Δ*zwf*	This study
ZF8	BAP1Δ*zwf*Δ*yihX*	This study
ZF9	BAP1Δ*pgi*Δ*yihX*	This study
ZF13	BAP1Δ*pgi*Δ*zwf*Δ*yihX*	This study
QC1	ZF1 carrying pBP130, pBP144, pZF230	This study
QC2	ZF2 carrying pBP130, pBP144, pZF230	This study
QC3	ZF3 carrying pBP130, pBP144, pZF230	This study
QC7	ZF7 carrying pBP130, pBP144, pZF230	This study
QC8	ZF8 carrying pBP130, pBP144, pZF230	This study
QC9	ZF9 carrying pBP130, pBP144, pZF230	This study
QC13	ZF13 carrying pBP130, pBP144, pZF230	This study
QC234	ZF13 carrying pBP130, pBP144, pZF234	This study
DTAC	ZF13 carrying pBP130, pBP144, pZF234, pACYC-dCas9-ter	This study
DT246	ZF13 carrying pBP130, pBP144, pZF234, pZF246	This study
DT239	ZF13 carrying pBP130, pBP144, pZF234, pZF239	This study

2. Materials and methods

2.1. Strains, plasmids and chemicals

E. coli DH10B was used for plasmid construction and the previously reported BAP1 [29] was used for the biosynthesis of polyketides EB and MEB. The compatible vectors pET21c and pCDFDuet-1 (Novagen, Germany) were used to express the heterologous gene of the TDP-L-mycarose. 4-(2-hydroxyethyl)-1-piperazi-neethanesuffonic acid (HEPES) used in fermentation was bought from Sangon (Shanghai). Authentic chemical standards 6-dEB, EB were prepared by our group. All restriction enzymes and DNA ligases were bought from NEB (New England Biolabs, USA).

2.2. Heterologous TDP-L-mycarose pathway construction and assembly

The plasmids related to TDP-L-mycarose were listed in Table 1. The TDP-L-mycarose pathway genes from *Saccharopolyspora erythraea* were previously constructed and stored by our lab. Genes *AeeryBIII* and *AeeryBVII* from *Aeromicrobium erythreum* were synthesized by Tongyong (Anhui, China) with codon optimization for *E. coli* (Table S1) and cloned into pET21c yielding plasmid pZF90 and pZF91. Gene *AeeryBIII* was then inserted into the pZF91 between the *Spe* I/*Sac* I to result in pZF92. The chaperone GroESL coding sequence was obtained through PCR with

the primers 224_F/R (Table S2) and the template pZF223, and then inserted into *Spe* I/*Sac* I site of pZF84 to generate pZF93.The pZF94 was generated by inserting the DNA fragment containing gene *eryBII* into pJF26 between *Spe* I/*Sac* I site. *SaeryBVI* and *SaeryBII* expression cassette was obtained by digestion pZF94 with restriction enzyme *Xba* I and *Sac* I, and then inserted into pZF93 between *Spe* I and *Sac* I to give pZF95. Subsequently, *SaeryBVII_SaeryBIII* and *AeeryBVII_AeeryBIII* expression cassettes were obtained by digesting pJF33 and pZF92 with restriction enzyme *Xba* I and *Sac* I, respectively, and then inserted into pZF95 between *Spe* I and *Sac* I to generate pZF227 and pZF228. Finally, the DNA fragment containing genes *SaeryBIV*, *SaeryBV* and *ermE* was obtained after the digestion of pJF37 with restriction enzyme *Xba* I and *Sac* I, and then constructed into pZF227 and pZF228, respectively, creating the corresponding pZF229 and pZF230 (Fig. S3).

2.3. CRISPR/Cas9-mediated knockout of chromosomal genes

The knockout of chromosomal genes in *E. coli* BAP1 was conducted by CRISPR/Cas9 system [30]. The sgRNA plasmid pZF9 was obtained from pCB003 by inverse PCR utilizing primer pairs pCB003_N20_pgi_F/R and its sequence was confirmed by sequencing. Similarly, other plasmids pZF10 and pZF11 were constructed with primers pCB003_N20_zwf_F/R and pCB003_N20_yihX_F/R, respectively (Table S2). The upstream (h1) and downstream (h2) homologous arms of the target genes (*pgi*, *zwf*, *yihX*) with the length of about 300-bp were separately amplified and then generated the donor DNA fragments by overlap PCR (Table S2). The PCR products were purified by gel extraction before electroporation. For the electroporation, 100 μL of *E. coli* BAP1 competent cells harboring pCB006 were prepared and mixed with 1000 ng donor DNA and 200 ng sgRNA plasmid. Electroporator (Bio--Rad, USA) was used for electroporation (1 cm cuvette, 1.8 kV). Cells were resuspended in 1 mL Luria Broth (LB) medium and recovered at 30 °C for 2 h before being plated onto LB agar containing kanamycin (50 mg/L) and spectinomycin (50 mg/L). The recombinant colonies were verified by colony PCR and DNA sequencing after incubating at 30 °C overnight. The individual colony edited successfully was inoculated into 2 mL of LB medium containing kanamycin (50 mg/L) and IPTG (0.5 mM) to cure the sgRNA plasmid, and the pCB006 could be eliminated when cell cultures were cultivated at 42 °C for 12 h.

2.4. Creation of plasmids for genes rfbA and rfbB overexpression

The *rfbA* and *rfbB* genes were amplified from the genomic DNA of *E. coli* BAP1 with primer pairs 225_rfbA_F/R, 225_rfbB_F/R (Table S2) and then fused by overlap PCR to generate *rfbAB*. The purified *rfbAB* fragments were assembled with pET21c treated with *Nde* I/*Hind* III using ClonExpress II One Step Cloning Kit (Vazyme, Nanjing, China), resulting in pZF225. The *rfbAB* expression cassette was amplified from template pZF225 with primer pairs FseI_rfbB/PacI_rfbA and then inserted into pZF230 under *Fse* I/*Pac* I sites to generate pZF234.

2.5. Construction of the CRISPRi-mediated system

For the construction of the L-arabinose-based CRISPRi system, the sgRNA cassette sequences were amplified using primers 236_vector_F/R (Table S2) from pZF208. The P_{ara} was amplified from pACYC-dCas9-Ter using primers 236_ara_F/R. These two PCR products were combined to make pZF236 using ClonExpress II One Step Cloning Kit (Vazyme, Nanjing, China). For the silencing of different endogenous genes (such as *rmlC*, *rfbD*, *pykA*, and *pykF*), the 20-bp guide sequences were obtained using predictions from ATUM's gRNA design tool (https://www.atum.bio/) and then inserted into pZF236 by PCR using primers 237_F/R, 238_F/R, 243_F/R, and 244_F/R (Table S2), generating four sgRNA plasmids pZF237, pZF238, pZF243, and pZF244. To produce vector pZF246 which express multiple guides and dCas9 under the control of individual P_{ara}, the pZF243 and pZF244 were used as templates to obtain the fragments which contain *Bsa* I restriction site using primers 246_rmlC_F/R and 246_rfbD_F/R. The *Bsa* I sites of pACYC-dCas9-Ter backbone were introduced by PCR using primers ACYC_F/R. Then, all fragments were digested with *Bsa* I (NEB, USA), and ligated to yield pZF246. The pZF237 and pZF238 were used as templates to obtain the fragments which contain *Bsa* I restriction site using primers 239_pykA_F/R and 239_pykF_F/R, then all fragments were digested with *Bsa* I (NEB, USA) and ligated to yield pZF239.

2.6. Media and culture conditions

Fermentation medium, LB (10 g/L tryptone, 5 g/L yeast extract, 10 g/L NaCl) supplemented with 15 g/L glycerol, 100 mM 4-(2-hydroxyethyl)-1-piperazi-neethanesuffonic acid (HEPES), was adjusted to pH 7.6 by NaOH before autoclaving and used to compare the production of engineering strains. For the biosynthesis of MEB, 100 μL of seed inoculum was inoculated into a 100 mL flask containing 10 mL fermentation medium supplemented with appropriate antibiotics (100 mg/L ampicillin, 50 mg/L kanamycin, 50 mg/L spectinomycin, and 34 mg/L chloramphenicol) and grown at 37 °C. Isopropyl β-D-thiogalactopyranoside (IPTG) and sodium propionate were added at a final concentration of 0.5 mM and 5 mM when OD_{600} reached 0.4. L-arabinose at a final concentration of 10 mM was added to induce the CRISPRi system when $OD_{600} = 2$. Cell cultures were subsequently incubated at 22 °C for 7 days.

2.7. HPLC and LC-MS/MS analytic methods

All samples were analyzed by high-performance liquid chromatography (HPLC) on an Ultimate 3000 HPLC system (ThermoFisher Scientific) with ELSD detector (Alltech U3000, Agilent) and a SilGreen ODS column (φ 4.6 × 250 mm, S-5 μm, Greenherbs, Beijing, China) maintained at 30 °C. Compounds were separated by acetonitrile (solvent A) and water (containing 50 mM ammonium formate, solvent B) at a flow rate of 1.0 mL/min under the following conditions: 0 min:100% B; 0–30 min: linear-gradient increase to 95% A in 5% B; 30–31 min: linear-gradient increase to100% B; 31–35 min: 100% B. The data shown in this study were generated from three independent experiments.

LC-MS/MS was performed on Q Exactive hybrid quadrupole-Orbitrap mass spectrometer (Thermo Scientific, MA, U.S.A.) equipped with Infinity Lab Poroshell 120 SB-AQ C18 column (φ 3.0 × 100 mm, 2.7 μm, Agilent, U.S.A.). The mobile phase was acetonitrile (A) and H_2O with 0.1% formic acid (B). A linear gradient was set as follows: 5–95% solvent A for 10 min; 95% solvent A for 1min; 95-5% solvent A for 5 min. The flow rate was 0.4 mL/min, and the injection volume was 2 μL. The mass acquisition was performed in positive ionization mode with a full scan (100–1000).

2.8. Purification and quantification of 3-O-α-mycarosylerythronolide B

To obtain high purity MEB, collected samples were first separated by column chromatography over SiliaSphere C18 (50 μm, Silicycle, QuébecK, QC, Canada), and then purified by semi-preparative HPLC (Dionex UltiMate 3000 Semi-Preparative HPLC Systems, Thermo Scientific, MA, U.S.A.) with 40% acetonitrile in water (flow rate of 10 mL/min, detected at 205 nm) and a SilGreen ODS C18 column (φ 20 × 250 mm, 5 μm, Greenherbs Co., Ltd., Beijing, China). ^{1}H and ^{13}C and 2D NMR spectra of MEB were recorded by an Avance DRX 400 (500 MHz for ^{1}H, 125 MHz for ^{13}C) spectrometer (Bruker, Germany). The standard curve of MEB was generated by calculating the peak area of MEB.

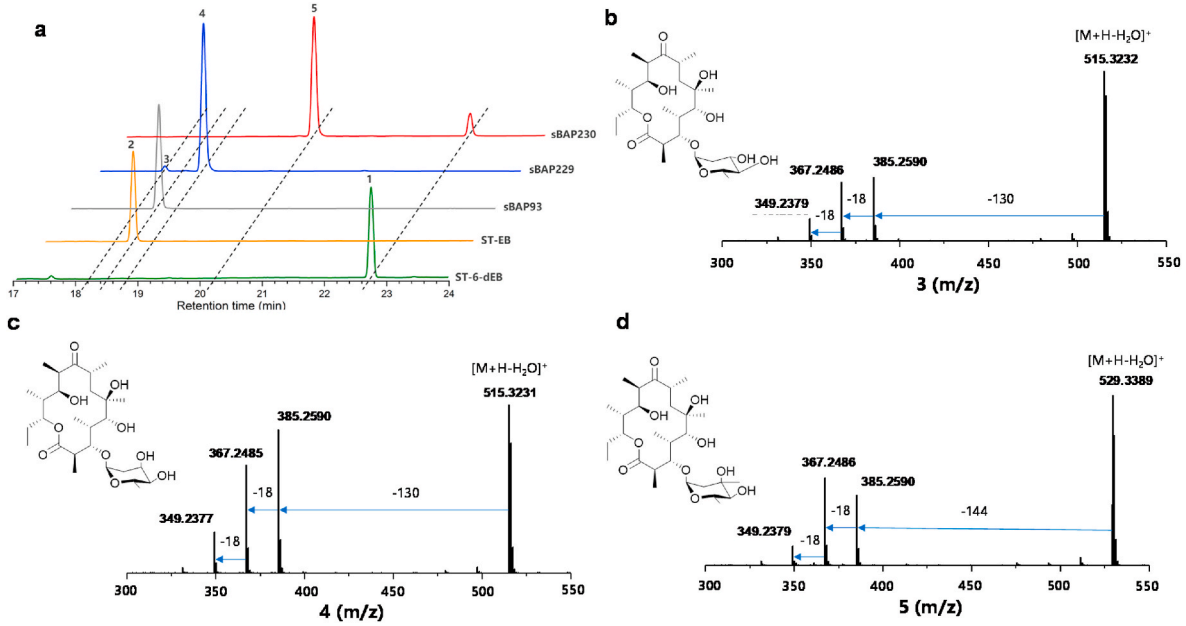

Fig. 2. The biosynthesis of 3-*O*-*α*-mycarosylerythronolide B (MEB) in *E. coli*. **a**, The HPLC analysis of the fermentation product of strains BAP229 (BAP1 harboring pBP130, pBP144, and pZF229) and BAP230 (BAP1 harboring pBP130, pBP144, and pZF230). ST-6-dEB, 6-dEB standard; ST-EB, EB standard; **1**, 6-dEB; **2**, EB; **3**, 3-*O*-(2″,6″-dideoxy-*α*-L-*arabino*-hexopyranosyl) erythronolide B; **4**: 3-*O*-(2″,6″-dideoxy-*α*-L-*ribo*-hexopyranosyl) erythronolide B; **5**: MEB; **b**, The LC-MS/MS fragments of compound **3**. **c**, The LC-MS/MS fragments of compound **4**. **d**, The LC-MS/MS fragments of compound **5**.

3. Results and discussion

3.1. Establishing the biosynthesis of 3-O-α-mycarosylerythronolide B in E. coli

To rebuild the biosynthesis of 3-*O*-*α*-mycarosylerythronolide B (MEB) in *E. coli*, the previously reported BAP1 harboring pBP130 and pBP144 was used as the starting strain (WT) to produce 6-dEB. Subsequently, we performed the expression analysis of the pathway genes of TDP-L-mycarose. As shown in Fig. S1, except for EryBIV and ErmE, the other six proteins could not be expressed. It has been demonstrated that the chaperones GroEL/GroES achieved the highest titer for MEB through improving the protein solubility when the TDP-L-mycarose operon was coexpressed with chaperones GroEL/GroES, GroEL/GroES/TIG, GrpE/DnaJ/DnaK, and GroEL/GroES/GrpE/DnaJ/DnaK, respectively [25]. Therefore, plasmid pZF93 was constructed by incorporating the chaperones GroEL/GroES into the previous hydroxylase SaEryF-expressing plasmid pZF84. All the genes involved in the biosynthesis and transfer of TDP-L-mycarose were cloned from *S. erythraea* and were assembled into plasmid pZF93 to generate pZF229. The recombinant strain BAP229 (transforming pZF229 into strain WT) was cultivated in shake flask for 168 h, together with strain BAP93 (introducing pZF93 into strain WT) being used as a control for TDP-L-mycarose biosynthesis. The precursor EB (**2**) was detected in the fermentation media of strain BAP93, whereas newly appeared compounds **3** (R_t = 18.2 min) and **4** (R_t = 18.8 min) were observed in the fermentation broth of BAP229 (Fig. 2a). The HPLC-MS/MS analysis indicated that compounds **3** and **4** might be the isomerized MEB derivatives lacking the C3′ methyl group according to the identical characteristic ion peaks of $[M + H–H_2O]^+$ (m/z = 515.3232), which was 14 mass units less than that of MEB (m/z = 529.3389) (Fig. 2b and c). A careful comparison of ^1H and ^{13}C NMR data of compounds **3** and **4** with those of **2** (Figs. S2–S7) suggested that **3** and **4** were the glycosylated derivatives of **2**. This deduction was supported by ^1H–^1H COSY cross-peaks of H1′/H2′/H3′/H4′/H5′/H6′ (δ_H 4.99/1.64/3.78/2.97/3.88/1.26 in **3**, and 4.98/1.95/3.96/3.26/4.15/1.28 in **4**) and the HMBC correlations from H1′ to C3 (δ_C 88.78 in **3**, and 88.36 in **4**) and C3′ (δ_C 69.39 in **3**, and 67.94 in **4**), H3′ to C2′ (δ_C 39.30 in **3**, and 36.39 in **4**), C4′ (δ_C 78.69 in **3**, and 73.51 in **4**) and C5′ (δ_C 70.20 in **3**, and 67.70 in **4**) as well as H6′ to C4′ and C5′ (Figs. S8–S15). The large coupling constants (J = 9.6 Hz) of H4′, H5′ and H6′ in **3** indicated that the substituents of C3′-C5′ are equatorial, while the small values of $^3J_{H1',H2'a}$ (3.0 Hz) and $^3J_{H2'a,H3'}$ (3.0 Hz) in **4** suggested that the substituents of C1′ and C3′ are axial. Therefore, compounds **3** and **4** were assigned as 3-*O*-(2″,6″-dideoxy-*α*-L-*arabino*-hexopyranosyl) erythronolide B and 3-*O*-(2″,6″-dideoxy-*α*-L-*ribo*-hexopyranosyl) erythronolide B, respectively, which were reported previously in the mutant *S. erythraea* [31].

We speculated that the generation of MEB derivatives instead of MEB might be attributed to the low enzymatic activity of SaeryBVII (TDP-4-keto-2,6-dideoxyhexose 3-*C*-methyltransferase) and SaeryBIII (TDP-4-deoxyglucose 3,5-epimerase). To verify this hypothesis, an assessment of protein expression of the pathway enzymes was conducted in *E. coli* BAP1 with the aid of chaperones GroEL/GroES. As we anticipated, with the exception of SaeryBVII and SaeryBIII, all TDP-L-mycarose pathway enzymes could be highly expressed (Fig. S16), which indicated that the soluble expression of eryBVII and eryBIII exerted an important effect on the biosynthesis of MEB.

To facilitate the creation of TDP-L-mycarose, the homologous AeeryBVII and AeeryBIII originated from *A. erythreum* were selected and synthesized with optimized codons. Protein expression analysis showed that both AeeryBVII and AeeryBIII gave distinct expression bands under the same cultivation condition (Fig. S17), which were utilized to replace the SaeryBVII and SaeryBIII of plasmid pZF229, resulting in plasmid pZF230 (Fig. S18). HPLC analysis clearly revealed the presence of 6-dEB (**1**) and a new compound **5** (R_t = 20.4 min) in the fermentation media of strain BAP230 generated by introducing pZF230 into strain WT (Fig. 2a). Compound **5** was subsequently identified as MEB by the characteristic ion peaks m/z 529.3389 observed in the HPLC-MS/MS mass profile and NMR spectra (Fig. 2d, S19 and S20). This result indicated the feasibility to achieve the biosynthesis of MEB in *E. coli* by combining pathway enzymes with effective expression. Eventually, the MEB concentration of BAP230 was quantified to be 4.2 mg/L on the basis of the established standard curve of MEB (Fig. S21).

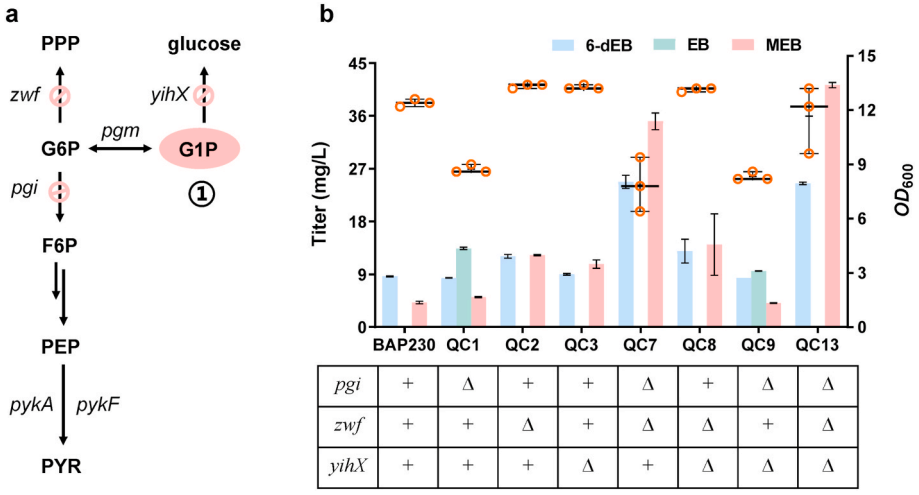

Fig. 3. Effects of the gene knockout on the cell growth and MEB production. **a**, The strategy 1 to enhance the MEB production by genes deletion. **b**, The 6-dEB, EB, and MEB production and OD_{600} of recombinant strains BAP230 (BAP1 harboring pBP130, pBP144, and pZF230), QC1 (ZF1 harboring pBP130, pBP144, and pZF230), QC2 (ZF2 harboring pBP130, pBP144, and pZF230), QC3 (ZF3 harboring pBP130, pBP144, and pZF230), QC7 (ZF7 harboring pBP130, pBP144, and pZF230), QC8 (ZF8 harboring pBP130, pBP144, and pZF230), QC9 (ZF9 harboring pBP130, pBP144, and pZF230) and QC13 (ZF13 harboring pBP130, pBP144, and pZF230).

3.2. Enhancing the 3-O-α-mycarosylerythronolide B production via pathway disruption

Given that the unusual sugar TDP-L-mycarose is the crucial biosynthetic bottleneck of MEB [28], it is essential to improve the yield of MEB by enhancing the intracellular TDP-L-mycarose pool. Glucose-6-phosphate (G6P) is the common precursor of glycolysis, pentose phosphate pathway and TDP-L-mycarose biosynthetic pathway. To provide more G6P for the synthesis of TDP-L-mycarose, glycolysis and pentose phosphate pathway that consume G6P need to be blocked. It has been demonstrated that deletion of genes *pgi* (encoding phosphoglucose isomerase) and *zwf* (encoding glucose-6-phosphate dehydrogenase) could improve the level of UDP-glucose and elevate the production of the corresponding glycosylated products [32–34]. Moreover, the G1P hydrolase encoded by gene *yihX* was capable of selectively hydrolyzing G1P, which is the intermediator of TDP-L-mycarose biosynthesis [35]. To reinforce the TDP-L-mycarose biosynthetic pathway and increase the MEB production, we individually knocked out genes *pgi*, *zwf*, and *yihX* in *E. coli* BAP1, generating strains ZF1(BAP1Δ*pgi*), ZF2(BAP1Δ*zwf*), and ZF3(BAP1Δ*yihX*) (Fig. 3a). Based on this, three plasmids pBP130, pBP144, and pZF230 responsible for the biosynthesis of MEB were introduced into ZF1, ZF2, and ZF3, respectively, yielding strains QC1, QC2, and QC3. QC2 and QC3 exhibited no growth defect compared with the parent strain BAP230 (OD_{600} = 13), while QC1 (OD_{600} = 8.7) was impaired to a certain extent. The parental strain BAP230 could produce 8.6 mg/L 6-dEB and 4.2 mg/L MEB with no detectable accumulation of EB, while the engineered QC2 and QC3 produced 12.3 mg/L and 10.7 mg/L MEB, a 2.9-fold and 2.5-fold to that produced by BAP230. Interestingly, the titer of MEB (5.1 mg/L) in QC1 was lower than QC2 and QC3, but it enabled the EB production to 13.4 mg/L EB (Fig. 3b). These results indicated that the single-gene knockout of the bypass pathway contributed to enhancing MEB production. Thus, we move on to investigate whether the combinatorial deletion of two genes could further elevate the MEB production. Three engineered strains QC7, QC8, and QC9 were subsequently constructed by introducing pBP130, pBP144, and pZF230 into strains ZF7 (BAP1Δ*pgi*Δ*zwf*), ZF8 (BAP1Δ*zwf*Δ*yihX*), and ZF9 (BAP1Δ*pgi*Δ*yihX*), respectively. As shown in Fig. 3b, the cell growth of QC7 (OD_{600} = 7.9) and QC9 (OD_{600} = 8.3) was similar to that

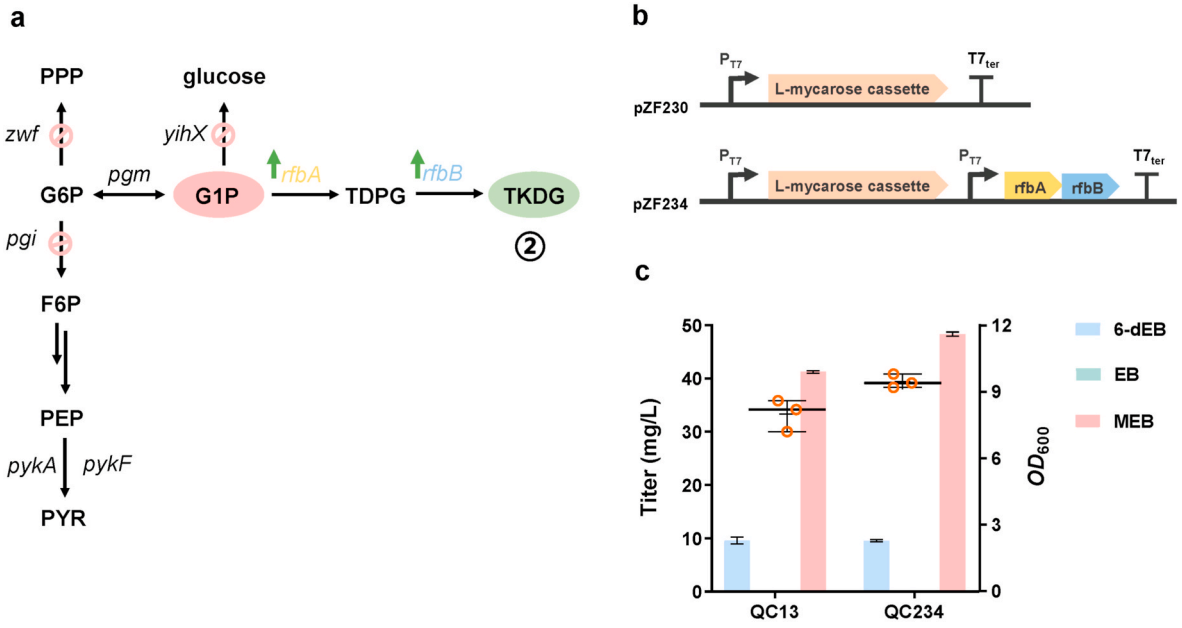

Fig. 4. The effects of overexpressing *rfbA* and *rfbB* on MEB production. **a**, The strategy 2 to reinforce the MEB production. **b**, Schematic diagram of pZF234. **c**, Cell growth and 6-dEB and MEB production of QC13 (ZF13 harboring pBP130, pBP144, and pZF230) and QC234 (ZF13 harboring pBP130, pBP144, and pZF234).

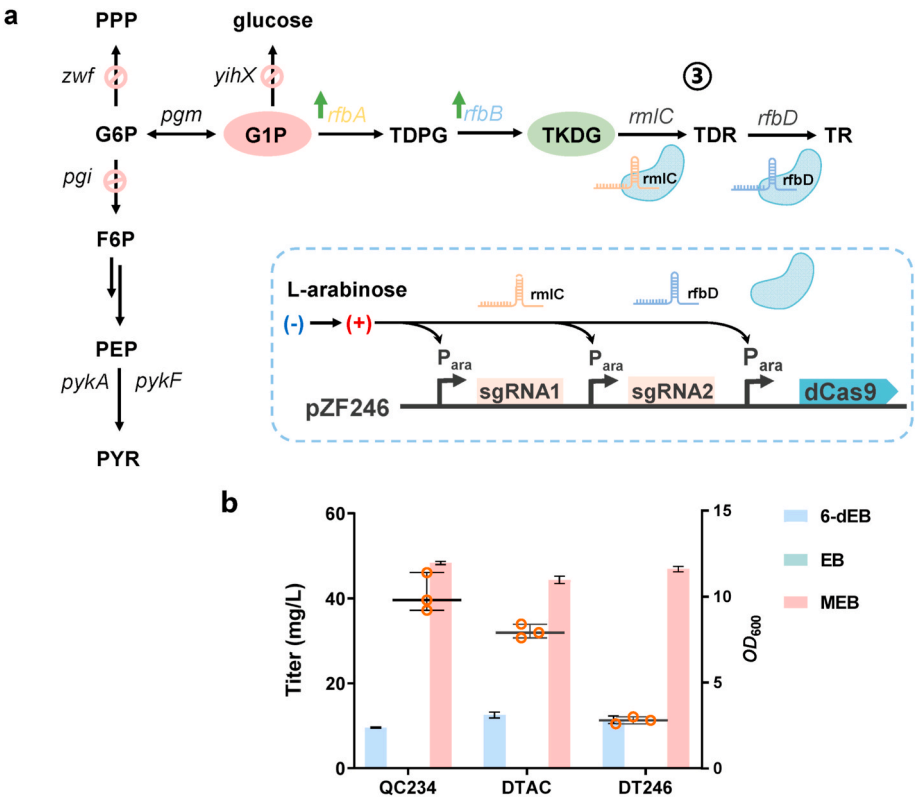

Fig. 5. Effects of CRISPRi targeting to *rmlC* and *rfbD* on MEB production. **a**, The strategy 3 to repress the TDP-L-rhamnose biosynthesis. **b**, The cell growth and production of 6-dEB, EB, and MEB of recombinant strains QC234 (ZF13 harboring pBP130, pBP144, and pZF234), DTAC (ZF13 harboring pBP130, pBP144, pZF234, and pACYC-dCas9-Ter), and DT246 (ZF13 harboring pBP130, pBP144, pZF234, and pZF246).

of strain QC1, while QC8 (OD_{600} = 13.1) showed no growth difference with wild-type strain BAP230. The 6-dEB and MEB concentrations in strain QC7 were 24.7 mg/L and 35.1 mg/L, increasing significantly by 190% and 740% compared to strain BAP230, respectively. The strain QC8 generated 12.9 mg/L 6-dEB and 14.0 mg/L MEB. Compared with strain BAP230, the titers of 6-dEB and MEB have no significant change accompanied with the accumulation of EB in strain QC9, suggesting that engineered *E. coli* drive more metabolic flux towards EB biosynthesis and the availability of endogenous TDP-L-mycarose was limited. Hence, we attempted to disrupt genes *pgi*, *zwf*, and *yihX* simultaneously and construct the recombinant strain ZF13 (BAP1Δ*pgi*Δ*zwf*Δ*yihX*) (Fig. S22). The corresponding fermentation strain QC13 afforded the highest MEB production with a titer of 41.2 mg/L, which is a 9.8-fold increase to that produced by BAP230. In addition, QC13 also achieved the highest production of 24.5 mg/L 6-dEB, which indicated the efficient downstream pathways utilizing 6-dEB as building unit or biosynthetic precursor might lead to the improved metabolic flux toward 6-dEB. These results suggested that increasing the carbon flux at the G1P node by blocking the competing pathway could drive the biosynthesis of TDP-L-mycarose and MEB. Therefore, strain ZF13 was chosen for further engineering.

3.3. Overexpression of *rfbA* and *rfbB* for 3-O-α-mycarosylerythronolide B production

Glucose-1-phosphate thymidylyltransferase (*rfbA*) and TDP-glucose-4,6-dehydratase (*rfbB*) are capable of converting G1P to TKDG, a crucial intermediate of TDP-L-mycarose (Fig. 4a). To further increase the MEB titer, we sought to reinforce the TDP-L-mycarose biosynthetic pathway via overexpression of *rfbA* and *rfbB*. Accordingly, the *rfbA_rfbB* module was cloned from *E. coli* and incorporated on the pZF230 as an independent operon, yielding plasmid pZF234 (Fig. 4b). The shake flask fermentation results showed that the MEB production of strain QC234 (ZF13 harboring pBP130, pBP144, pZF234) was slightly increased and reached a maximum of 48.3 mg/L, a 17% increase relative to strain QC13 (41.2 mg/L). Intriguingly, strain QC234 produced 9.6 mg/L of 6-dEB, which is comparable to that of QC13 (Fig. 4c).

To verify whether the increase in MEB yield was due to the enhancement of TDP-L-mycarose, we measured the cellular concentration of TDP-L-mycarose in the engineered strains that exclusively synthesize the sugar skeleton. As shown in Fig. S23, the triple knockout strain sZF13 (pZF230) that was engineered to enhance the supply of G1P was capable of producing 107.2 mg/L TDP-L-mycarose, a 12.9-fold to that of the control strain BAP1 (pZF230) (8.3 mg/L), while the sZF13 (pZF234) which was created to enhance the supply of G1P and further convert the precursor G1P into the key intermediator TKDG achieved the highest titer of TDP-L-mycarose of 143.3 mg/L, a 16.3-fold increase to that produced by BAP1 (pZF230).

3.4. Regulating the metabolic pathway of *E. coli* with CRISPRi

Considering that genes overexpression involved in TDP-L-mycarose pathway led to a modest increase in MEB production, which might be due to the leakage of TKDG caused by TDP-L-rhamnose synthesis and the shortage of intracellular G1P, we next aim to improve MEB titer by addressing these problems. TDP-4-dehydrorhamnose-3,5-epimerase (*rmlC*) and TDP-L-rhamnose synthase (*rfbD*) were reported to catalyze TKDG to form TDP-L-rhamnose that played pivotal roles in membrane synthesis and cellular function [36]. To mitigate the leakage of TKDG, we implemented the CRISPRi system mediated by P_{ara} promoter in the established strain QC234 to downregulate the expression of these two endogenous genes *rmlC* and *rfbD* (Fig. 5a). Consequently, pZF246 was constructed by inserting two sgRNA cassettes targeting *rmlC* and *rfbD* into the dCas9-expressing plasmid pACYC-dCas9-Ter (Fig. S24a).

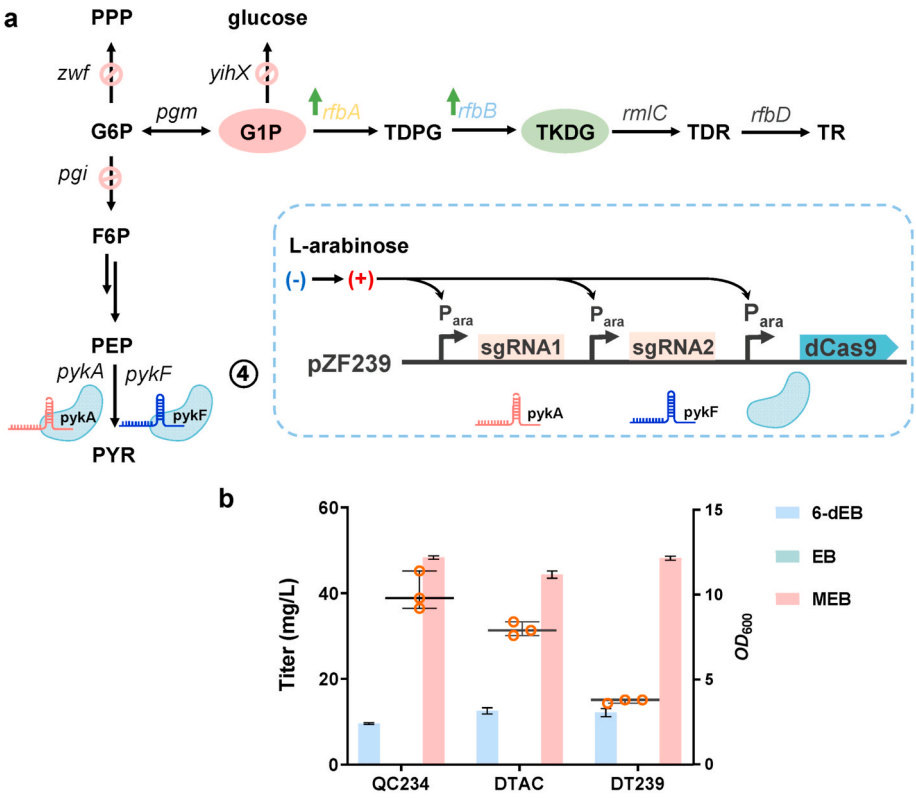

Fig. 6. Effects of CRISPRi targeting to *pykA* and *pykF* on MEB production. **a**, The strategy 4 to repress the glycolysis pathway. **b**, The cell growth and production of 6-dEB, EB, and MEB of recombinant strains QC234 (ZF13 harboring pBP130, pBP144, and pZF234), DTAC (ZF13 harboring pBP130, pBP144, pZF234, and pACYC-dCas9-Ter), and DT239 (ZF13 harboring pBP130, pBP144, pZF234, and pZF239).

Introduction of the pACYC-dCas9-Ter and pZF246 into the efficient MEB producer QC234 resulted in recombinant strain DTAC and DT246, respectively. Unexpectedly, the repression of TDP-L-rhamnose biosynthesis in strain DT246 (OD_{600} = 2.8) resulted in striking growth defect compared with strain QC234 (OD_{600} = 10.1) (Fig. 5b), whereas strain DTAC (OD_{600} = 8.0) showed slightly impaired growth. The reason that the titers of MEB in strains DTAC (44.4 mg/L) and DT246 (46.9 mg/L) were decreased could be ascribed to the compromised cell growth. Despite the application of CRISPRi exhibited no beneficial effects on MEB production, the MEB concentration per OD_{600} of DT246 was 3.5-fold to that of QC234.

Pyruvate kinases II (*pykA*) and I (*pykF*) are indispensable enzymes in the glycolysis pathway which have been widely investigated and engineered to rewire the carbon metabolism and facilitate the generation of nucleotide-activated sugar donor [34,37]. To further promote the formation of G1P, we thus reconstructed the CRISPRi system to reduce the expression of *pykA* and *pykF* by replacing the sgRNAs of pZF246, yielding pZF239 (Fig. S24b), which was transformed into strain QC234 to obtain DT239 (Fig. 6a). Although a slightly recovered cell growth was observed in DT239 (OD_{600} = 3.7) in comparison with DT246, simultaneous inhibition of *pykA* and *pykF* failed to accomplish the improvement of MEB production in strain DT239 (48.2 mg/L), nearly equal to the titer of QC234 (48.3 mg/L) (Fig. 6b). This might largely be attributable to the metabolite burden caused by the expression of multiple pathway genes and transcriptional regulators. In spite of the fact that the implementation of the CRISPRi resulted in no remarkable increase in the concentration of MEB, the higher biomass specific rate of MEB still demonstrated the functionality of CRISPRi system in driving carbon flux from G1P to TDP-L-mycarose.

4. Conclusions

In summary, the multi-level metabolic engineering approach including gene disruption, gene overexpression and CRISPRi was successively performed to achieve high-level TDP-L-mycarose and boost MEB production. Notably, the strain QC234 producing 48.3 mg/L MEB and 9.6 mg/L 6-dEB, was constructed by deletion of *pgi*, *zwf*, and *yihX* and overexpression of *rfbA* and *rfbB*. The CRISPRi system was employed to repress bypass pathways that consume precursors, leading to a 250% increase in the titer of MEB per OD_{600} in DT246 compared with QC234. This study lays the foundation for de novo biosynthesis of erythromycin and other glycosylated products decorated by unusual sugar.

CRediT authorship contribution statement

Zhifeng Liu: Conceptualization, Methodology, Software, Validation, Visualization, Writing – original draft, Writing – review & editing. **Jianlin Xu:** Methodology, Software, Validation, Writing – original draft, Writing – review & editing. **Zhanguang Feng:** Methodology, Software. **Yong Wang:** Project administration, Funding acquisition, Supervision.

Declaration of competing interest

The authors declare no competing financial interest.

Acknowledgements

This study was financially supported by the National Key R&D Program of China (2018YFA0900600), the Program of Shanghai Academic Research Leader (20XD1404400), the Strategic Priority Research

Program “Molecular mechanism of Plant Growth and Development” of CAS (XDB27020202), the National Natural Science Foundation of China (31670099), the Construction of the Registry and Database of Bioparts for Synthetic Biology of the Chinese Academy of Science (No. ZSYS-016), the International Partnership Program of Chinese Academy of Science (No. 153D31KYSB20170121) and the National Key Laboratory of Plant Molecular Genetics, SIPPE, CAS.

Appendix A. Supplementary data

Supplementary data to this article can be found online at https://doi.org/10.1016/j.synbio.2022.03.002.

References

[1] Cao HZ, Hwang J, Chen X. Carbohydrate-containing natural products in medicinal chemistry. In: Opportunity, challenge and scope of natural products in medicinal chemistry; 2011. p. 411–31.
[2] Wu L, Georgiev MI, Cao H, Nahar L, El-Seedi HR, Sarker SD, Xiao J, Lu B. Therapeutic potential of phenylethanoid glycosides: a systematic review. Med Res Rev 2020;40:2605–49.
[3] Mrudulakumari Vasudevan U, Lee EY. Flavonoids, terpenoids, and polyketide antibiotics: role of glycosylation and biocatalytic tactics in engineering glycosylation. Biotechnol Adv 2020;41:107550.
[4] Weymouth-Wilson AC. The role of carbohydrates in biologically active natural products. Nat Prod Rep 1997;14:99–110.
[5] Xiao J. Dietary flavonoid aglycones and their glycosides: which show better biological significance? Crit Rev Food Sci Nutr 2017;57:1874–905.
[6] Xiao J, Capanoglu E, Jassbi AR, Miron A. Advance on the flavonoid C-glycosides and health benefits. Crit Rev Food Sci Nutr 2016;56:S29–45.
[7] Xu JL, Liu ZF, Zhang XW, Liu HL, Wang Y. Microbial oligosaccharides with biomedical applications. Mar Drugs 2021;19:350.
[8] Fang L, Zhang G, El-Halfawy O, Simon M, Brown ED, Pfeifer BA. Broadened glycosylation patterning of heterologously produced erythromycin. Biotechnol Bioeng 2018;115:2771–7.
[9] Thibodeaux CJ, Melancon CE, Liu HW. Natural-product sugar biosynthesis and enzymatic glycodiversification. Angew Chem Int Ed Engl 2008;47:9814–59.
[10] Zhang G, Li Y, Fang L, Pfeifer BA. Tailoring pathway modularity in the biosynthesis of erythromycin analogs heterologously engineered in *E. coli*. Sci Adv 2015;1:e1500077.
[11] Madduri K, Kennedy J, Rivola G, Inventi-Solari A, Filippini S, Zanuso G, Colombo AL, Gewain KM, Occi JL, MacNeil DJ, Hutchinson CR. Production of the antitumor drug epirubicin (4′-epidoxorubicin) and its precursor by a genetically engineered strain of *Streptomyces peucetius*. Nat Biotechnol 1998;16:69–74.
[12] Brown KV, Wandi BN, Metsä-Ketelä M, Nybo SE. Pathway engineering of anthracyclines: blazing trails in natural product glycodiversification. J Org Chem 2020;85:12012–23.
[13] De Bruyn F, Van Brempt M, Maertens J, Van Bellegem W, Duchi D, De Mey M. Metabolic engineering of *Escherichia coli* into a versatile glycosylation platform: production of bio-active quercetin glycosides. Microb Cell Factories 2015;14:138.
[14] Feng Y, Yao M, Wang Y, Ding M, Zha J, Xiao W, Yuan Y. Advances in engineering UDP-sugar supply for recombinant biosynthesis of glycosides in microbes. Biotechnol Adv 2020;41:107538.
[15] Huang FC, Hinkelmann J, Hermenau A, Schwab W. Enhanced production of beta-glucosides by in-situ UDP-glucose regeneration. J Biotechnol 2016;224:35–44.
[16] Xu P, Ranganathan S, Fowler ZL, Maranas CD, Koffas MA. Genome-scale metabolic network modeling results in minimal interventions that cooperatively force carbon flux towards malonyl-CoA. Metab Eng 2011;13:578–87.
[17] Simkhada D, Lee HC, Sohng JK. Genetic engineering approach for the production of rhamnosyl and allosyl flavonoids from *Escherichia coli*. Biotechnol Bioeng 2010;107:154–62.
[18] Bi HP, Qu G, Wang S, Zhuang YB, Sun ZT, Liu T, Ma YH. Biosynthesis of a rosavin natural product in *Escherichia coli* by glycosyltransferase rational design and artificial pathway construction. Metab Eng 2021;69:15–25.
[19] Chen A, Gu N, Pei J, Su E, Duan X, Cao F, Zhao L. Synthesis of isorhamnetin-3-*O*-rhamnoside by a three-enzyme (rhamnosyltransferase, glycine max sucrose synthase, UDP-rhamnose synthase) cascade using a UDP-rhamnose regeneration system. Molecules 2019;24:3042.
[20] Pei J, Dong P, Wu T, Zhao L, Fang X, Cao F, Tang F, Yue Y. Metabolic engineering of *Escherichia coli* for astragalin biosynthesis. J Agric Food Chem 2016;64:7966–72.
[21] Zabala D, Brana AF, Florez AB, Salas JA, Mendez C. Engineering precursor metabolite pools for increasing production of antitumor mithramycins in *Streptomyces argillaceus*. Metab Eng 2013;20:187–97.
[22] Zabala D, Brana AF, Salas JA, Mendez C. Increasing antibiotic production yields by favoring the biosynthesis of precursor metabolites glucose-1-phosphate and/or malonyl-CoA in *Streptomyces producer* strains. J Antibiot (Tokyo) 2016;69:179–82.
[23] Zhou X, Wu H, Li Z, Zhou X, Bai L, Deng Z. Over-expression of UDP-glucose pyrophosphorylase increases validamycin A but decreases validoxylamine A production in *Streptomyces hygroscopicus* var. jinggangensis 5008. Metab Eng 2011;13:768–76.
[24] Liu ZF, Xu JL, Liu HL, Wang Y. Engineered EryF hydroxylase improving heterologous polyketide erythronolide B production in *Escherichia coli*. Microb Biotechnol 2022. https://doi.org/10.1111/1751-7915.14000.
[25] Peirú S, Menzella HG, Rodriguez E, Carney J, Gramajo H. Production of the potent antibacterial polyketide erythromycin C in *Escherichia coli*. Appl Environ Microbiol 2005;71:2539–47.
[26] Zhang H, Wang Y, Wu J, Skalina K, Pfeifer BA. Complete biosynthesis of erythromycin A and designed analogs using *E. coli* as a heterologous host. Chem Biol 2010;17:1232–40.
[27] Jiang M, Fang L, Pfeifer BA. Improved heterologous erythromycin A production through expression plasmid re-design. Biotechnol Prog 2013;29:862–9.
[28] Peiru S, Rodriguez E, Menzella HG, Carney JR, Gramajo H. Metabolically engineered *Escherichia coli* for efficient production of glycosylated natural products. Microb Biotechnol 2008;1:476–86.
[29] Pfeifer BA, Admiraal SJ, Gramajo H, Cane DE, Khosla C. Biosynthesis of complex polyketides in a metabolically engineered strain of *E. coli*. Science 2001;291:1790–2.
[30] Jiang Y, Chen B, Duan C, Sun B, Yang J, Yang S. Multigene editing in the *Escherichia coli* genome via the CRISPR-Cas9 system. Appl Environ Microbiol 2015;81:2506–14.
[31] Collum P, Egan RS, Goldstein AW, Martin JR. 3-*O*-(2″,6″-dideoxy-*α*-L-ribo-hexopyranosyl)-erythronolide B and 3-*O*-(2″,6″,dideoxy-*α*-L-arabino-hexopyranosyl)erythronolide B, aberrant erythromycin biogenetic metabolites with defective sugar moities. Tetrahedron 1976;32:2375–8.
[32] Malla S, Pandey RP, Kim BG, Sohng JK. Regiospecific modifications of naringenin for astragalin production in *Escherichia coli*. Biotechnol Bioeng 2013;110:2525–35.
[33] Pandey RP, Malla S, Simkhada D, Kim BG, Sohng JK. Production of 3-*O*-xylosyl quercetin in *Escherichia coli*. Appl Microbiol Biotechnol 2013;97:1889–901.
[34] Wu Y, Sun X, Lin Y, Shen X, Yang Y, Jain R, Yuan Q, Yan Y. Establishing a synergetic carbon utilization mechanism for non-catabolic use of glucose in microbial synthesis of trehalose. Metab Eng 2017;39:1–8.
[35] Pfeiffer M, Wildberger P, Nidetzky B. Yihx-encoded haloacid dehalogenase-like phosphatase HAD4 from *Escherichia coli* is a specific alpha-D-glucose 1-phosphate hydrolase useful for substrate-selective sugar phosphate transformations. J Mol Catal B Enzym 2014;110:39–46.
[36] Marolda CL, Feldman MF, Valvano MA. Genetic organization of the O7-specific lipopolysaccharide biosynthesis cluster of *Escherichia coli* VW187 (O7:K1). Microbiology 1999;145(Pt 9):2485–95.
[37] Meza E, Becker J, Bolivar F, Gosset G, Wittmann C. Consequences of phosphoenolpyruvate:sugar phosphotranferase system and pyruvate kinase isozymes inactivation in central carbon metabolism flux distribution in *Escherichia coli*. Microb Cell Factories 2012;11:127.